Electronic Supplementary Material (ESI) for New Journal of Chemistry.

$Mo_{10}V_2$@MIL-101: Pseudo-capacitive and Redox-active Efficient Anode Material for High-rate Lithium Cluster Batteries

Marimuthu Priyadarshini[a], Swaminathan Shanmugan[a], Chang Woo Lee[b], and Kumaran Vediappan*[a]*

[a]Electrochemical Energy Storage and Conversion Laboratory (EESCL), Department of Chemistry, Faculty of Engineering and Technology, SRM Institute of Science and Technology, Kattankulathur-603203, Tamil Nadu, India.

[b]Department of Chemical Engineering and Green Energy Centre, College of Engineering, Kyung Hee University, 1 Seochun, Gihung, Yongin 446-701, Republic of Korea

E-mail: shanmugs2@srmist.edu.in, kumaranv@srmist.edu.in

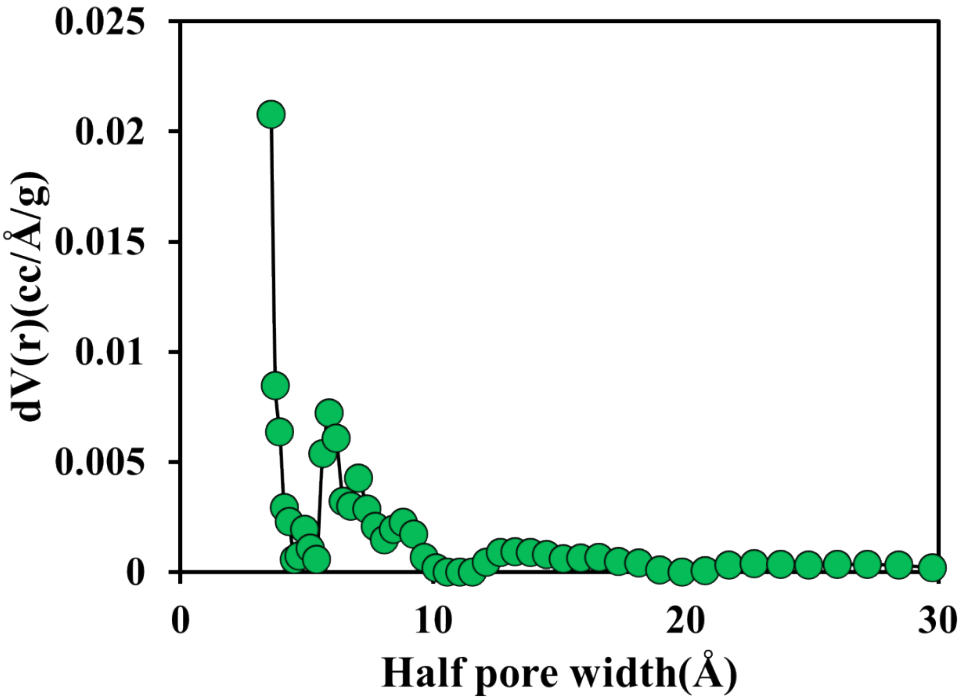

Figure. S1 Pore size distribution of $Mo_{10}V_2$@MIL-101.

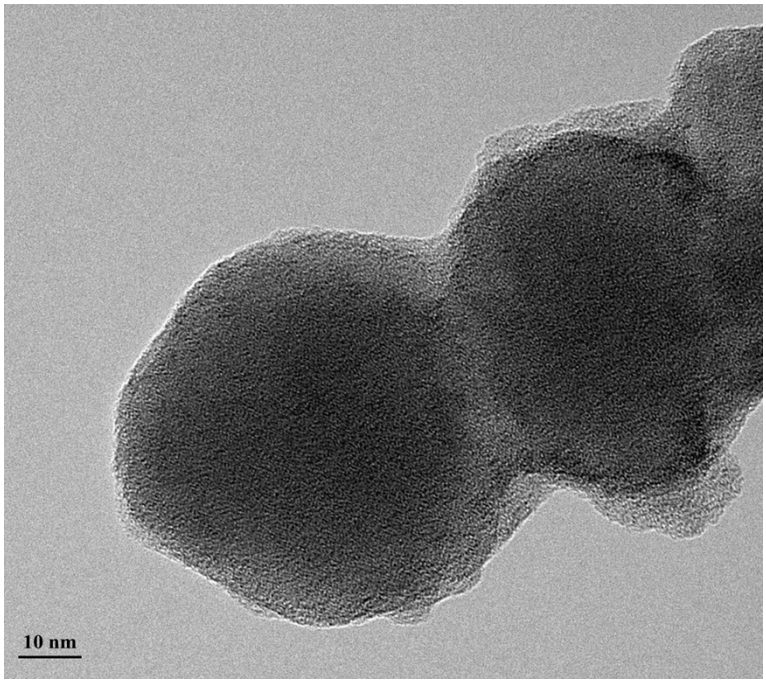

Figure. S2 HRTEM image of $Mo_{10}V_2$.

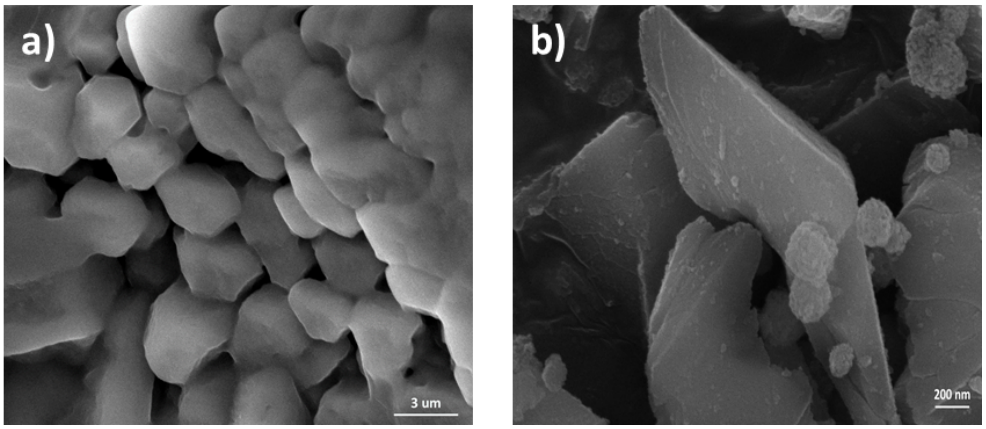

Figure. S3 FESEM images of $Mo_{10}V_2$@MIL-101 a) top view, b) side view.

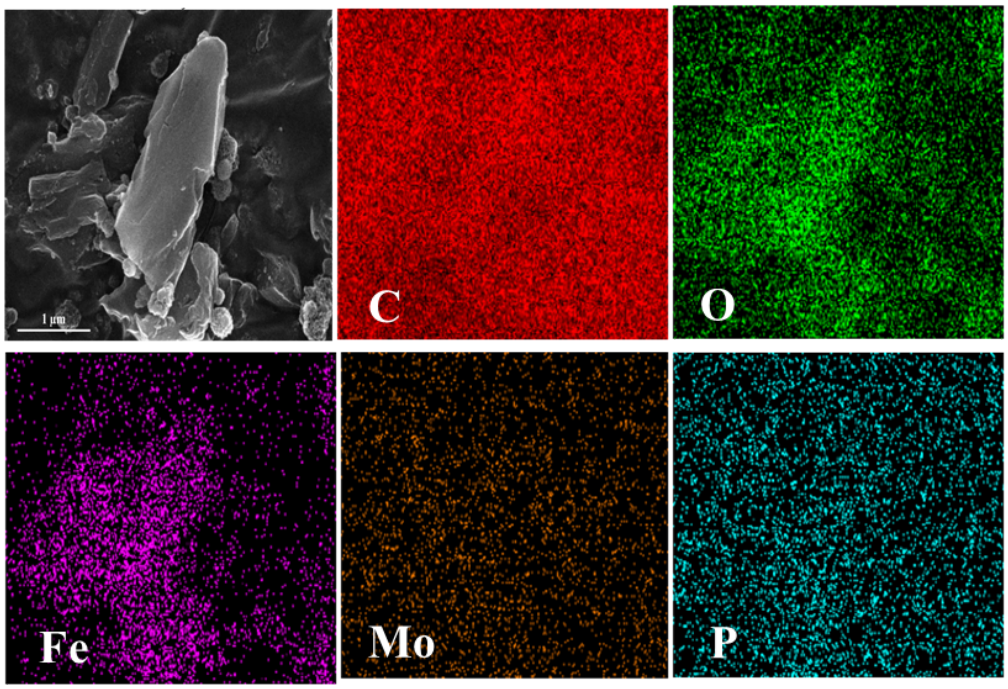

Figure. S4 FESEM image of $Mo_{10}V_2$@MIL-101 and the corresponding elemental mapping: red, green, violet, brown and blue indicates carbon, oxygen, iron, molybdenum and phosphorus.

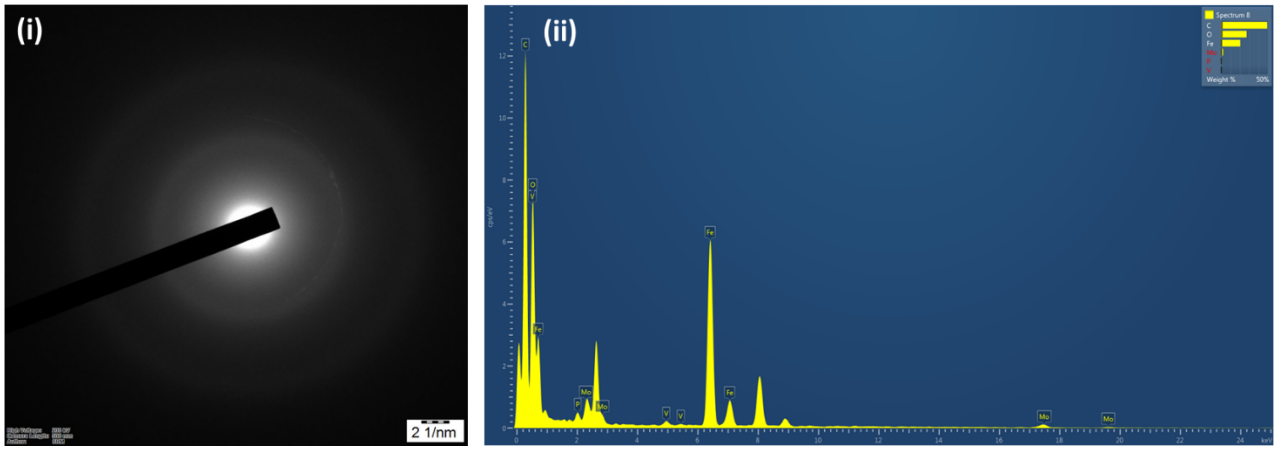

Figure. S5 i) Electron diffraction pattern and ii) HRTEM EDAX of $Mo_{10}V_2$@MIL-101

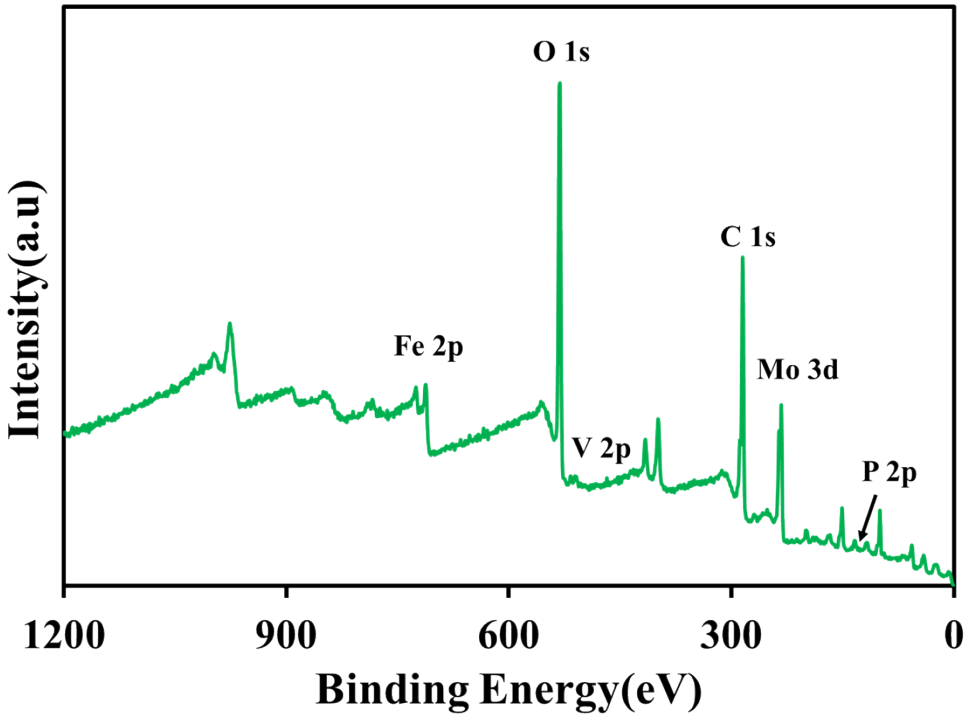

Figure. S6 XPS survey spectra of $Mo_{10}V_2$@MIL-101.

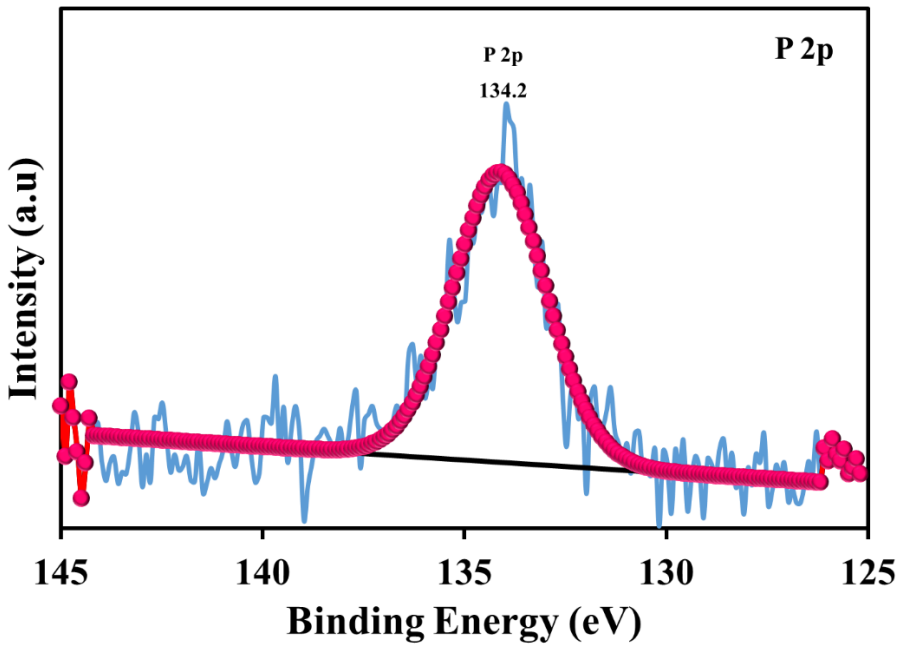

Figure. S7 XPS High resolution spectra P of $Mo_{10}V_2$@MIL-101.

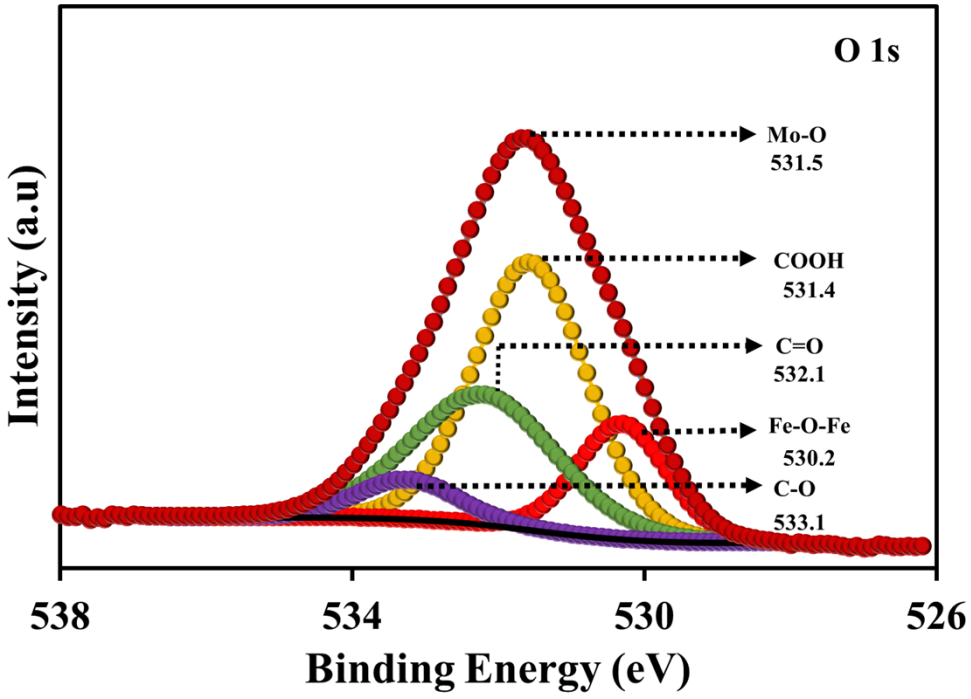

Figure. S8 XPS High resolution spectra O of $Mo_{10}V_2$@MIL-101.

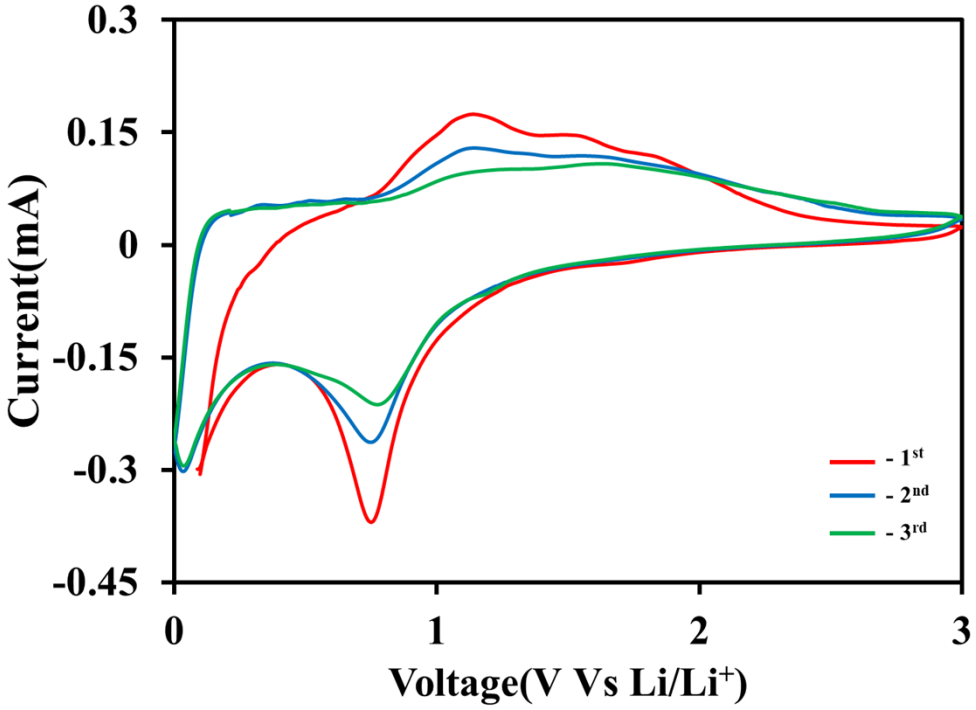

Figure. S9 CV of MIL-101(Fe) between the potential window 0.0-3.0V at a scan rate of 0.1 mV s^{-1}.

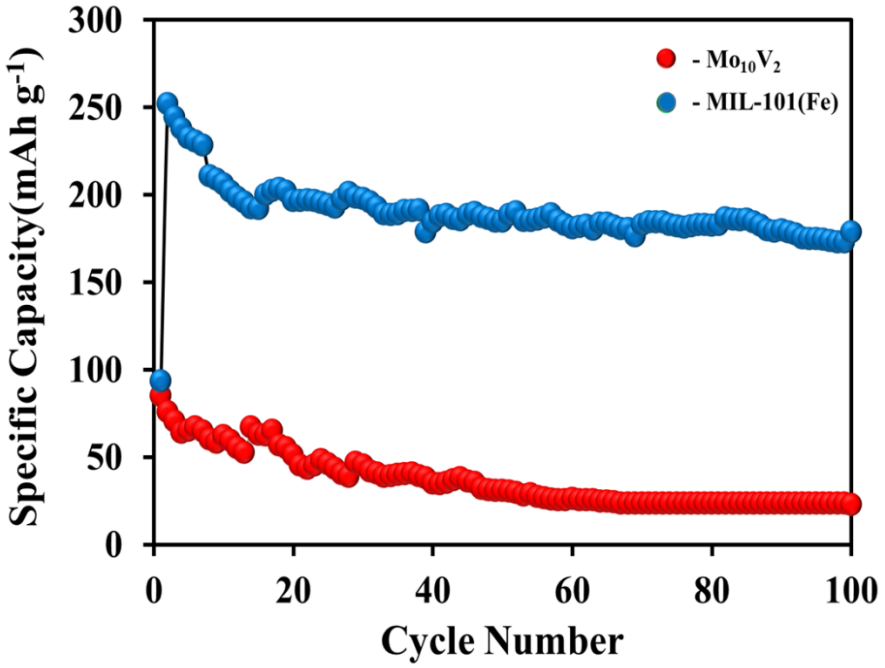

Figure. S10 Life cycle performance of $Mo_{10}V_2$ and MIL-101(Fe) at 1000 mA g^{-1}.

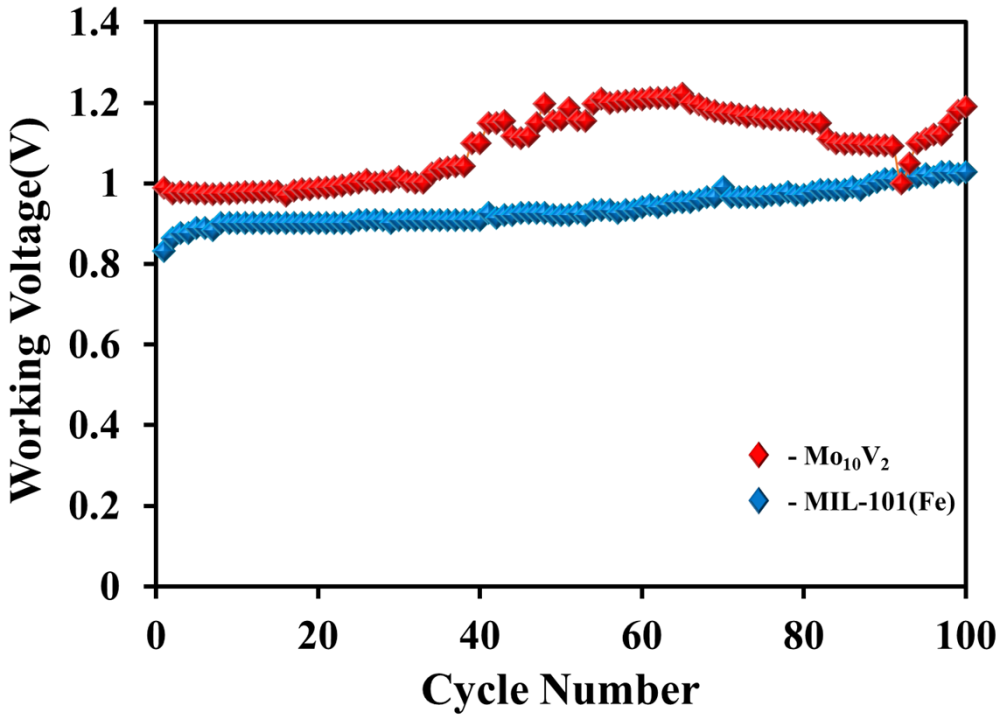

Figure. S11 Cycle number Vs Working voltage of $Mo_{10}V_2$ and MIL-101(Fe).

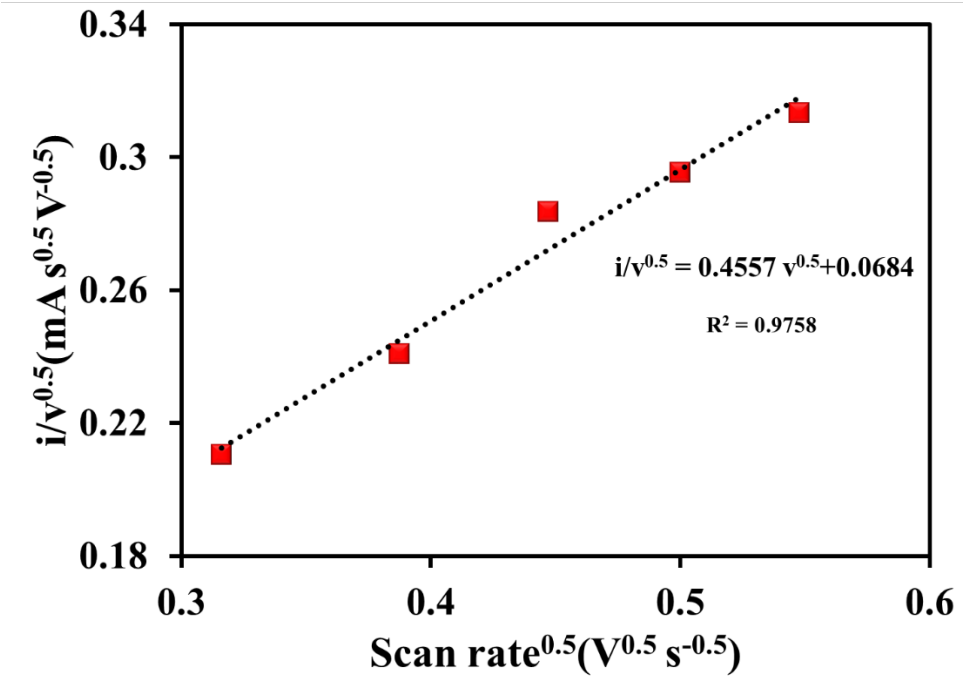

Figure S12. Linear fitting of plot of i/υ1/2 versus υ1/2 for first oxidation-reduction peak and second oxidation reduction peak.

Table 1. Comparison of charge/discharge capacity of various POM@MOF and POMOF compounds with this work

Material	Rate/CD (C/mA g^{-1})	RC (mAh g^{-1})	Cycles	CE (%)	Ref
POMOF-1	1.25 C	350	500	62.2	[1]
$[Ag_{26}(Trz)_{16}(OH)_4][P_2W_{18}O_{62}]$	100	550	100		
$Na[Ag_{16}(Trz)_9(H_2O)_4][P_2W_{18}O_{62}].H_2O$	100	600	100		[2]
$[PMoV_8Mo^{VI}_4O_{37}(OH)_3Zn_4][TPT].2TPT.2H_2O$	50	750	200	61.3	[3]
$(TBA)_3[PMoV_8Mo^{VI}_4O_{38}(OH)_2Zn_4(PBA)_2].H_2O$	100	640	100	56.2	[4]
POMOFs/RGO	50	1075	400		[5]
CoW-MO10V2	100	737	100	72	[6]
PMo_{12}@FeBTC	100	658	50	49.0	[7]
$H_2[Cu^{II}_4(Htrz)_5(H_2O)_2][Mo^{VI}_4Cu^{II}_4O_{26}]_{0.5}\cdot 3H_2O$	100	700	100	53	[8]
$[Cu_{24}(Trz)_{16}(H_2O)Cl_4(HPMo_{12}O_{40})]$	100	525	200	68	[9]
$Cu_4(bte)_4(\beta\text{-}Mo_8O_{26})$	100	575	100	40.4	[10]
$Mo_{10}V_2$@MIL-101	100	725	100	82	This
	1000	625	300	88	work

CD = Current density, RC = Reversible capacity, CE = Coulombic efficiency (Initial)

References

(1) Yue, Y.; Li, Y.; Bi, Z.; Veith, G. M.; Bridges, C. A.; Guo, B.; Chen, J.; Mullins, D. R.; Surwade, S. P.; Mahurin, S. M.; et al. A POM-Organic Framework Anode for Li-Ion Battery. *J. Mater. Chem. A* **2015**, *3* (45), 22989–22995.

(2) Li, M.; Cong, L.; Zhao, J.; Zheng, T.; Tian, R.; Sha, J.; Su, Z.; Wang, X. Self-Organization towards Complex Multi-Fold Meso-Helices in the Structures of Wells-Dawson Polyoxometalate-Based Hybrid Materials for Lithium-Ion Batteries. *J. Mater. Chem. A* **2017**, *5* (7), 3371–3376.

(3) Huang, Q.; Wei, T.; Zhang, M.; Dong, L. Z.; Zhang, A. M.; Li, S. L.; Liu, W. J.; Liu, J.; Lan, Y. Q. A Highly Stable Polyoxometalate-Based Metal-Organic Framework with π-π Stacking for Enhancing Lithium Ion Battery Performance. *J. Mater. Chem. A* **2017**, *5* (18), 8477–8483.

(4) Wang, Y. Y.; Zhang, M.; Li, S. L.; Zhang, S. R.; Xie, W.; Qin, J. S.; Su, Z. M.; Lan, Y. Q. Diamondoid-Structured Polymolybdate-Based Metal-Organic Frameworks as High-Capacity Anodes for Lithium-Ion Batteries. *Chem. Commun.* **2017**, *53* (37), 5204–5207.

(5) Wei, T.; Zhang, M.; Wu, P.; Tang, Y. J.; Li, S. L.; Shen, F. C.; Wang, X. L.; Zhou, X. P.; Lan, Y. Q. POM-Based Metal-Organic Framework/Reduced Graphene Oxide Nanocomposites with Hybrid Behavior of Battery-Supercapacitor for Superior Lithium Storage. *Nano Energy* **2017**, *34*, 205–214.

(6) Sun, K.; Li, H.; Ye, H.; Jiang, F.; Zhu, H.; Yin, J. 3D-Structured Polyoxometalate Microcrystals with Enhanced Rate Capability and Cycle Stability for Lithium-Ion Storage. *ACS Appl. Mater. Interfaces* **2018**, *10* (22), 18657–18664.

(7) Meng, X.; Wang, H. N.; Zou, Y. H.; Wang, L. S.; Zhou, Z. Y. Polyoxometalate-Based Metallogels as Anode Materials for Lithium Ion Batteries. *Dalt. Trans.* **2019**, *48* (28),

(8) Zhu, P.; Yang, X.; Li, X.; Sheng, N.; Zhang, H.; Zhang, G.; Sha, J. Insights into the Lithium Diffusion Process in a Defect-Containing Porous Crystalline POM@MOF Anode Material. *Dalt. Trans.* **2019**, *49* (1), 79–88.

(9) Yang, X.; Zhu, P.; Ma, X.; Li, W.; Tan, Z.; Sha, J. Graphite-like Polyoxometalate-Based Metal-Organic Framework as an Efficient Anode for Lithium Ion Batteries. *CrystEngComm* **2020**, *22* (8), 1340–1345.

(10) Wang, Z.; Bi, R.; Liu, J.; Wang, K.; Mao, F.; Wu, H.; Bu, Y.; Song, N. Polyoxometalate-Based Cu/Zn-MOFs with Diverse Stereo Dimensions as Anode Materials in Lithium Ion Batteries. *Chem. Eng. J.* **2021**, *404*.